Relating the optical absorption coefficient of nanosheet dispersions to the intrinsic monolayer absorption

Keith R. Paton* and Jonathan N. Coleman

School of Physics and CRANN & AMBER Research Centres, Trinity College Dublin, Dublin 2, Ireland

**patonk@tcd.ie*

Abstract: The concentration of nanosheet suspensions is an important technological parameter which is commonly measured by optical spectroscopy, using the absorption coefficient to transform absorbance into concentration. However, for all 2D materials, the absorption coefficient is poorly known, resulting in potentially large errors in measured concentration. Here we derive an expression relating the optical absorption coefficient of an isotropic dispersion of nanosheets to the intrinsic monolayer absorption. This has allowed us to calculate the absorption coefficients for suspensions of graphene, MoS_2 and other 2D materials, and to estimate the monolayer absorption for new materials from careful measurement of the suspension absorption coefficient.

1. Introduction

Liquid phase exfoliation of layered materials has become one of the most widely used methods to obtain nanosheets in an easily processable form[1-8]. Nanosheet suspensions (a.k.a. dispersions or inks) have been shown to be ideally suited to production of printed electronics[9, 10], including devices such as LEDs, battery and supercapacitor electrodes[11-16], photo-detectors[17] and hydrogen evolution catalysts[18-23], as well as additives in composites[23-26]. While the production of these dispersions can be scaled to industrial levels[8], methods to reliably and rapidly characterise the material produced are limited. Measurement of the concentration of nanosheets in the dispersion is commonly achieved by optical absorption spectroscopy, through the application of the Beer-Lambert Law. Note that we use the term nanosheets throughout this paper to refer to objects consisting of 1 or more monolayers (generally fewer than 10), where for some materials (e.g. MoS_2) a monolayer may be more than one atom thick. While this has been widely used for a range of nanosheet dispersions, it

requires an accurate value for the absorption coefficient (or more usefully the extinction coefficient[27]). This in turn is usually obtained by removing the liquid from the dispersion, either by filtering or evaporation, and weighing the resulting solid (taking account of any surfactant or solvent residues). Despite the simplicity of the procedure to obtain this important parameter, the values reported in the literature vary widely, from as low as 1043 $ml \cdot mg^{-1} \cdot m^{-1}$ to as high as 6600 $ml \cdot mg^{-1} \cdot m^{-1}$ for graphene[28, 29]. Similar variation exists for other 2D materials such as MoS_2 (see SI). It is not clear which papers are correct, as theoretical values of the suspension absorption coefficient are not available.

However, this is a problem which should be easily addressed. For a number of 2D materials, notably graphene, the amount of incident light absorbed by a single monolayer is known experimentally. This intrinsic material property is the primary factor controlling the absorption coefficient of a dispersion of nanosheets. Once it is known, it should be straightforward to derive a relationship between these quantities. However, to date such a calculation has not been published. In the present paper, we derive an expression relating the absorption coefficient for dispersions of nanosheets to the optical absorption of a monolayer at normal incidence. This relationship will allow the calculation of dispersion absorption coefficients from theoretical estimates of monolayer absorption and the validation of experimental values of absorption coefficient. In addition, it will be possible to estimate the monolayer absorption from careful measurements of dispersion absorption coefficient.

2. Results and Discussion

Optical spectrometers physically measure the transmission of light, T (defined as the ratio of transmitted, I, to incident, I_0, light intensity). However, the data is often outputted as the absorbance, which we will refer to here as A_T. In the absence of scattering (see below), this parameter is generally defined as $A_T = -\log_{10} T$ and it is this quantity that is automatically outputted by the spectrometer software (i.e. not $-\ln T$)[30]. The absorbance is useful because it is directly proportional to the quantity of absorbing material: $A_T = \alpha CL$ where C is the concentration of nanosheets, defined as the dispersed mass/dispersion volume. Although more typically applied to liquid solutions, with absorbing species truly dissolved in a solvent, it has been shown by several authors that it can also be applied to samples of 2D nanosheets dispersed in solvents [1, 29, 31-34]. Here the proportionality constant, α, is the absorption coefficient which tends to be poorly known (L is the cell length, the distance the beam travels through the vessel containing the liquid).

The simplest way to calculate α is via the absorption, A, which (in the absence of scattering) is the fractional light intensity change as the beam travels through the sample: $A=(T_0-T)/T_0$, where T_0 is transmission in the absence of the sample. Neglecting reflections, we have $A=1-T$. For a dilute solution, where αCL is small, it is straightforward to show that $A=\alpha CL/\log_{10} e$, where *e*=2.72. Thus, calculation of the absorbance will allow us to find the absorption coefficient (see SI for full derivation).

The absorption of a dispersion of nanosheets is simply the sum of the absorptions of all individual 2D nanosheets. To calculate this we must consider that, at any given instant, the nanosheets are randomly distributed throughout the liquid with isotropic orientation distribution. To calculate the total absorption, we consider a nanosheet whose orientation is defined by the polar angle, θ, and azimuthal angle, ϕ, associated with the unit vector normal to its basal plane, $\hat{\mathbf{n}}$ (see Figure 1A). The contribution to the absorption from all nanosheets with this orientation is given by

$$dA = A_{NS}(\theta,\phi)N_\Omega d\Omega \quad (1)$$

where $A_{NS}(\theta,\phi)$ is the absorption of a single nanosheet of this orientation, N_Ω is the number of nanosheets per unit solid angle and $d\Omega$ is the differential solid angle defined by θ and ϕ, given by $d\Omega=\sin\theta d\theta d\phi$ (Figure 1B). N_Ω is the total number of nanosheets interacting with the beam, multiplied by the fraction of nanosheets per unit solid angle. The latter parameter is the nanosheet orientation distribution function, Γ_{NS}, which for an isotropic distribution is given by $\Gamma_{NS}=1/2\pi$ (see SI). This allows us to write $N_\Omega = N_V\Lambda_{Beam}L/2\pi$ where N_V is the number of nanosheets per unit volume, Λ_{Beam} is the area of the beam in the x-y plane, and L is the cell length. This parameter can be written in terms of the nanosheet concentration:

$$N_\Omega = \frac{C\,\Lambda_{Beam}L}{2\pi\rho_{NS}\Lambda_{NS}t_{NS}} \quad (2)$$

where ρ_{NS}, Λ_{NS} and t_{NS} are the nanosheet density, area and thickness respectively.

This allows us to write the total absorption of the dispersion as

$$A = \frac{C\,\Lambda_{Beam} L}{2\pi \rho_{NS}\,\Lambda_{NS} t_{NS}} \int_{\theta=0}^{\pi} \int_{\phi=0}^{\pi} A_{NS}(\theta,\phi)\sin\theta\, d\theta d\phi \quad (3)$$

where the upper limits of integration are π because of the planar symmetry of the nanosheet, with absorption equivalent regardless of the direction of light propagation through the basal plane[REF]. We therefore require an expression for $A_{NS}(\theta,\phi)$, the absorption of the single nanosheet.

The value of A_{NS} varies with orientation for two main reasons. Firstly, the projected area the nanosheet presents to the beam depends on nanosheet orientation and, secondly, the amount of light the nanosheet absorbs depends on the square of the cosine of the angle between the nanosheet basal plane and the electric field vector of the light (essentially Malus' law, see SI).

The fraction of the total light intensity absorbed by a single nanosheet is given by the fraction of beam area occluded by the nanosheet, F_Λ, multiplied by the fraction of light intensity incident on the nanosheet that is absorbed. This second parameter is given by $A_{\|}\cos^2\gamma$, where $A_{||}$ is the intrinsic nanosheet absorption (i.e. when the electric field of the light is parallel to the nanosheet basal plane) and γ is the angle between the electric field vector and the basal plane of the nanosheet (see figure 1C). Combining these gives

$$A_{NS}(\theta,\phi) = F_\Lambda(\theta,\phi) A_{\|}\cos^2\gamma(\theta,\phi) \quad (4)$$

We will now address $F_\Lambda(\theta,\phi)$, $A_{\|}$ and $\gamma(\theta,\phi)$ separately.

The parameter $F_\Lambda(\theta,\phi)$ represents the fraction of total beam area occluded by a nanosheet whose orientation is described by θ and ϕ. This is simply the projection of the nanosheet area onto the plane perpendicular to the propagation direction of the light (in this case the x-y plane)[35] and is given by

$$F_\Lambda(\theta,\phi) = \frac{\Lambda_{NS}}{\Lambda_{Beam}}\cos\Psi \quad (5)$$

where Ψ is the angle between the basal plane of the nanosheet and the x-y plane. It can be shown (see SI) that $\cos\Psi = \sin\theta\sin\phi$, giving

$$F_{\Lambda}(\theta,\phi)=\frac{\Lambda_{NS}}{\Lambda_{Beam}}\sin\theta\sin\phi \quad (6)$$

The intrinsic absorption of the nanosheet is represented by $A_{\parallel}$, which describes the fractional reduction in intensity for light incident on the nanosheet. For a thin nanosheet comprised of N layers, this is approximately (see SI) given by

$$A_{\parallel}=NA_{ML} \quad (7)$$

where A_{ML} is the intrinsic absorption of a monolayer (when the electric field vector is in the plane of the nanosheet). This parameter is defined by the electronic properties of the monolayer and is known for a number of materials (see below), for example $A_{ML}\approx 2.3\%$ for graphene at wavelengths >400 nm[36].

The amount of light absorbed by the nanosheet depends on the angle between the plane of the nanosheet and the electric field vector, $\gamma(\theta,\phi)$. This depends on both the orientation of the nanosheet (described by θ and ϕ) and the direction of the electric field vector which we take as being in the x-y plane at an angle of β to the x-axis (see Figure 1C). In the present analysis, we consider the 2D nanosheets to be rigid, and ignore any bending or folding that may be present. However, we feel that folding of flakes is unlikely to be present in a stable dispersion of 2D nanosheets. The bending of nanosheets is also expected to be a dynamic process, such that the shape to be approximated to a rigid object on the timescale of any measurement. Then, it can be shown (see SI) that

$$\cos^2\gamma(\theta,\phi)=1-\cos^2\theta\cos^2\beta-\sin^2\theta\cos^2\phi\sin^2\beta-2\cos\theta\sin\theta\cos\phi\cos\beta\sin\beta \quad (8)$$

We can combine expressions (4) - (8), recalling that $A=\alpha CL/\log_{10}e$ to give an equation for the absorption coefficient of the nanosheet dispersion:

$$\alpha=\frac{\log_{10}e}{2\pi\rho_{NS}d_0}A_{ML}\int_{\theta=0}^{\pi}\int_{\phi=0}^{\pi}\cos^2\gamma(\theta,\phi)\sin\theta\sin\phi\sin\theta\,d\theta\,d\phi \quad (9)$$

Here, we have used $t_{NS}=Nd_0$, where d_0 is the monolayer thickness, and for brevity have not substituted $\cos^2\gamma$ from equation 8. Performing the integration reduces this equation to

$$\alpha(\lambda)=\frac{3\log_{10}e}{8\rho_{NS}d_0}A_{ML}(\lambda) \quad (10)$$

In this expression, we explicitly show that both $\alpha(\lambda)$ and $A_{ML}(\lambda)$ are usually functions of wavelength. We note that equation 10 is not a function of β, as expected for an isotropic nanosheet distribution. This shows that the absorption coefficient is polarisation independent. It is also important to note that the absorption coefficient is not predicted to depend on the lateral flake size or thickness. However, as discussed below, for some materials A_{ML} is a function of flake size as well as wavelength.

Having derived an expression relating the measured absorption coefficient (α) to the intrinsic nanosheet absorption (A_{ML}) we can now apply this to dispersions of nanosheets where A_{ML} is known. This is simplest for graphene, where it has been shown that $A_{ML,Gra}$ =0.023 for wavelengths between ~400 nm and ~800 nm. Substituting this value into equation 10 gives a predicted value of α_{Gra} =4237 ml.mg^{-1}m^{-1}, which is close to the centre of the range of experimental values reported (see figure 2). Very recently, we carefully measured the absorption coefficient of graphene dispersions finding α_{750}=4,861 Lg^{-1}m^{-1}, in very good agreement with the theoretical value[37].

The monolayer absorption for MoS_2 has been measured recently, and shown to be strongly wavelength dependent[38]. This is in agreement with measured absorbance spectra of dispersions of this materials, where variation is also found with flake size[27, 39]. This flake size dependence has been shown to be the result of the edge region having a different value of A_{ML} from the basal plane. Therefore, equation 10 is only strictly valid at the specific wavelength where $A_{ML,basal} = A_{ML,edge}$. For MoS_2 it has been shown that this occurs at ~345 nm, which is a local minimum in the absorption spectrum[27]. At this local minimum, monolayer MoS_2 has a measured $A_{ML} = 0.07$, allowing us to calculate a predicted value for the absorption coefficient of $\alpha_{MoS_2}(336nm) = 3631\ ml\ \cdot mg^{-1}m^{-1}$. Comparing this to the reported values in figure 2 we find that this predicted value is within the range of experimental values, albeit at the low end of the range.

We can carry out similar analysis for other layered materials exfoliated as nanosheets, such as WS_2, $MoSe_2$ and WSe_2, where values of A_{ML} have been measured experimentally. Taking the value at the local minimum, where it is assumed that $A_{ML,basal} = A_{ML,edge}$, we can predict the absorption coefficient for dispersions of these materials. These predicted values are shown in table 1, which in the case of WS_2 we have compared to reported experimental values in figure 2.

We can also use equation 10 to estimate the monolayer absorption for 2D materials where this is not known. Using an integrating sphere, the absorption coefficient of GaS suspensions has been shown to be nanosheet-size-independent at 365 nm (very close to the bandedge, considerably below the peak absorption) with a value of $\alpha_{GaS}\approx300$ ml.mg^{-1}m^{-1}. Taking the density as ρ_{NS}=3860 kg/m^3 and $d_0\approx0.5$ nm, we get $A_{ML}(\lambda=365nm)\approx0.0036$. This value is rather low because the wavelength chosen is so close to the bandedge.

However, care must be taken when comparing absorption coefficients predicted by equation 10 to literature values (and *vice versa*). This is because the equation relating absorbance to transmission given above ($A_T = -\log_{10} T$), although widely used, is not strictly correct for dispersed nanoparticles due to the presence of light scattering. In an optical spectrometer, light is lost from the beam via both absorption and scattering. While for molecular systems the scattering component is generally negligible, for nanomaterials this is not the case. In such systems the measured transmittance is related to the extinction coefficient, ε, ($-\log_{10} T = \varepsilon CL$) which includes contributions from both absorption and scattering such that $\varepsilon(\lambda) = \alpha(\lambda) + \sigma(\lambda)$ (where σ is the scattering coefficient)[27]. For 2D nanosheets such as those considered here, the scattering spectrum is difficult to predict, both sue to shape effects, and the possibility that edge regions may exhibit different scattering behaviour from centre of the flakes. Depending on the concentration of nanosheets in the dispersion, there may also be multiple scattering events, further complicating the process.

While these contributions can be separated using an integrating sphere to give the true value of α this is not widely done. Thus, the vast majority of papers that report values of the absorption coefficient are actually reporting the extinction coefficient. This means most literature values purporting to be the absorption coefficient, but actually giving the extinction coefficient, would be expected to be larger than the theoretical value. Careful measurements of ε, α and σ for MoS_2 and graphene have shown that $\alpha/\varepsilon\sim0.7$-0.9[27, 37]. However, we note that this may not always be the case in practice because of the significant experimental errors associated with measuring the extinction coefficient. It is also important to note that the magnitude of the scattering component may be dependent on the size of the 2D nanosheets, as has been shown by Backes *et al* for MoS_2 nanosheets[27].

When using equation 10 therefore, it must be kept in mind that it represents the absorption rather than the extinction coefficient. This limits how it can be applied. The ideal approach would be to measure the absorption coefficient for the material under study in an

integrating sphere and compare directly with the theoretical value. Failing that it would be possible to use the fact that the extinction coefficient is generally 10-30% higher than the absorption coefficient in the resonant region[27, 37]. Applying this would allow the estimation of the extinction coefficient from the theoretical absorption coefficient. Such a procedure would allow estimations of nanosheet concentrations with acceptable accuracy.

While measuring neglecting the scattering contribution will lead to overestimation of the absorption coefficient, it is no such obvious explanation for underestimation. One source may be a failure to account properly for solvent or surfactant residues when determining the mass of dispersed 2D nanosheets. Such dispersions are typically stabilised by high boiling point solvents, what can be difficult to fully remove, or surfactant molecules, which will remain bound to the flakes. If these residues are not accounted for, then the apparent mass of nanosheets will be overestimated, leading to an underestimation of the absorption coefficient, as any contribution to the absorbance of the sample will be removed by baseline subtraction. It is also possible that some of the experimental results were measured from dispersions in which the concentration of dispersed nanosheets was too high. The Beer-Lambert Law is only valid for reasonably dilute solutions (or, in this case, dispersions), with an underestimation resulting from high concentration samples. Again, this would result in value for α that is lower than the true value.

Although we have assumed an isotropic orientation distribution of flakes within the dispersion, it would be straightforward to substitute an alternative expression for Γ_{NS}. While for reasonably dilute dispersions, this would not be necessary, in certain systems it may be more appropriate, such as thin films or reinforced polymers. In such systems, any alignment may be introduced as a side-effect of the production/deposition method, or deliberately in order to enhance, for example, mechanical reinforcement or electrical conductivity. Indeed, it is possible that such an analysis, using polarised light, could be used to measure the orientation of 2D nanosheets within such a sample.

3. Conclusion

In conclusion, we have derived an expression to calculate the value for the absorption coefficient for dispersions of nanosheets, we have provided a benchmark to compare experimental values of the important characterisation parameter. While the optical absorption of monolayers has only been reported for a few of these materials, the expression can be applied

to new materials as they are measured. By providing a theoretical value for the absorption coefficient, it is hoped that the current wide spread of experimental values will begin to narrow.

The research leading to these results has received funding from the European Union Seventh Framework Program under grant agreement n°604391 Graphene Flagship. We have also received support from the Science Foundation Ireland (SFI) funded centre AMBER (SFI/12/RC/2278**).** In addition, JNC acknowledges the European Research Council (SEMANTICS) and SFI (11/PI/1087) for financial support.

Figures

Table 1: Predicted value of absorption coefficient, α, using equation 10 and references[36] and [38].

Material	**A_{ML} (%)**	**λ (nm)**	**α (ml mg^{-1} m^{-1})**
Graphene	2.3 [36]	400-800	4237
MoS2	14.87 [38]	336	7719
WS2	9.79 [38]	315	3429
MoSe2	4.62 [38]	380	1661
WSe2	10.05[38]	383	2702

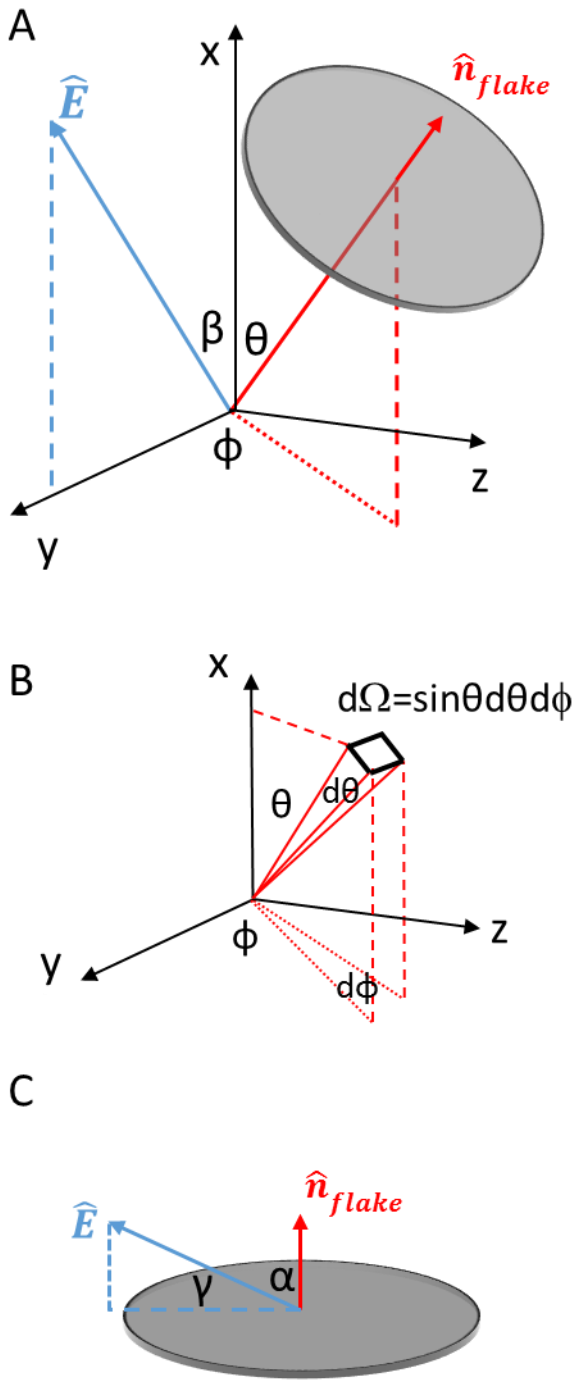

Figure 1: A) Diagram showing geometry of flake orientation. Light is taken to propagate in the z-direction, with electric field vector making an angle β with the x-axis. The normal to the flake makes an angle θ with the x-axis, and ϕ with the y-axis. The flake is shown as offset from the origin for clarity. B) Schematic showing the construction of the differential solid angle $d\Omega$. C) Diagram showing angle between the flake and electric field vector of the light.

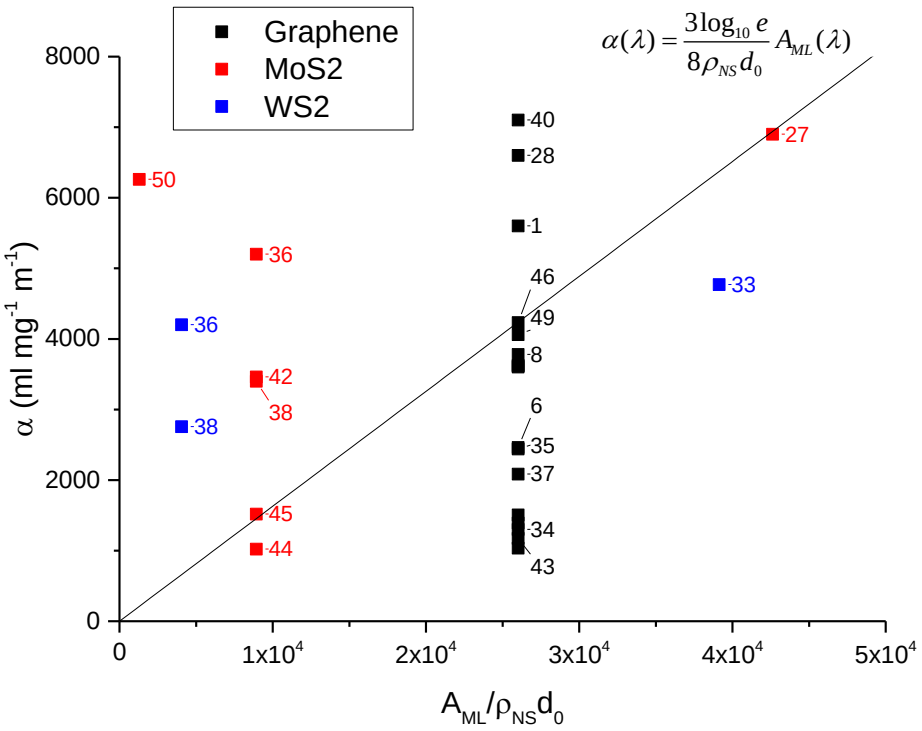

Figure 2: Reported values of absorption coefficient for dispersions of graphene (black squares), MoS_2 (red triangles) and WS_2 (blue circles). These have been plotted against the calculated value of $A_{ML}/(\rho_{NS} d_0)$ with the value for A_{ML} taken from ref [36] and [38] at the same wavelength as the experimental value. Note that for all the values for graphene dispersions, the value of A_{ML} has been taken from the region of the spectra where this is wavelength independent. For MoS_2 and WS_2 there is no such region, and so A_{ML} varies with wavelength. The line shows equation 10. [1, 6, 8, 27-29, 31-34, 39-52]

References

[1] N. Behabtu, J.R. Lomeda, M.J. Green, A.L. Higginbotham, A. Sinitskii, D.V. Kosynkin, D. Tsentalovich, A.N.G. Parra-Vasquez, J. Schmidt, E. Kesselman, Y. Cohen, Y. Talmon, J.M. Tour, M. Pasquali, Spontaneous high-concentration dispersions and liquid crystals of graphene., Nature nanotechnology 5 (2010) 406-11.
[2] V. Chabot, B. Kim, B. Sloper, C. Tzoganakis, A. Yu, High yield production and purification of few layer graphene by gum arabic assisted physical sonication., Scientific reports 3 (2013) 1378.
[3] J.N. Coleman, Liquid exfoliation of defect-free graphene., Accounts of chemical research 46 (2013) 14-22.
[4] L. Dong, S. Lin, L. Yang, J. Zhang, C. Yang, D. Yang, H. Lu, Spontaneous exfoliation and tailoring of MoS2 in mixed solvents., Chemical communications (Cambridge, England) 50 (2014) 15936-9.
[5] A.A. Green, M.C. Hersam, Solution phase production of graphene with controlled thickness via density differentiation., Nano letters 9 (2009) 4031-6.
[6] Y. Hernandez, V. Nicolosi, M. Lotya, F.M. Blighe, Z. Sun, S. De, I.T. McGovern, B. Holland, M. Byrne, Y.K. Gun'Ko, J.J. Boland, P. Niraj, G. Duesberg, S. Krishnamurthy, R. Goodhue, J. Hutchison, V. Scardaci, A.C. Ferrari, J.N. Coleman, High-yield production of graphene by liquid-phase exfoliation of graphite., Nature nanotechnology 3 (2008) 563-8.
[7] V. Nicolosi, M. Chhowalla, M.G. Kanatzidis, M.S. Strano, J.N. Coleman, Liquid Exfoliation of Layered Materials, Science 340 (2013) 1226419-1226419.
[8] K.R. Paton, E. Varrla, C. Backes, R.J. Smith, U. Khan, A. O'Neill, C. Boland, M. Lotya, O.M. Istrate, P. King, T. Higgins, S. Barwich, P. May, P. Puczkarski, I. Ahmed, M. Moebius, H. Pettersson, E. Long, J. Coelho, S.E. O'Brien, E.K. McGuire, B.M. Sanchez, G.S. Duesberg, N. McEvoy, T.J. Pennycook, C. Downing, A. Crossley, V. Nicolosi, J.N. Coleman, Scalable production of large quantities of defect-free few-layer graphene by shear exfoliation in liquids., Nature materials 13 (2014) 624-30.
[9] F. Torrisi, J.N. Coleman, Electrifying inks with 2D materials., Nature nanotechnology 9 (2014) 738-739.
[10] F. Torrisi, T. Hasan, W. Wu, Z. Sun, A. Lombardo, T.S. Kulmala, G.-W. Hsieh, S. Jung, F. Bonaccorso, P.J. Paul, D. Chu, A.C. Ferrari, Inkjet-printed graphene electronics., ACS nano 6 (2012) 2992-3006.
[11] M.a. Bissett, I.A. Kinloch, R.A.W. Dryfe, Characterization of MoS 2 –Graphene Composites for High-Performance Coin Cell Supercapacitors, ACS Applied Materials & Interfaces (2015) 150731121859008.
[12] I.-W.P. Chen, Y.-S. Chen, N.-J. Kao, C.-W. Wu, Y.-W. Zhang, H.-T. Li, Scalable and high-yield production of exfoliated graphene sheets in water and its application to an all-solid-state supercapacitor, Carbon 90 (2015) 16-24.
[13] D. Hanlon, C. Backes, T.M. Higgins, M. Hughes, A. O'Neill, P. King, N. McEvoy, G.S. Duesberg, B. Mendoza Sanchez, H. Pettersson, V. Nicolosi, J.N. Coleman, Production of Molybdenum Trioxide Nanosheets by Liquid Exfoliation and Their Application in High-Performance Supercapacitors, Chemistry of Materials 26 (2014) 1751-1763.
[14] T.M. Higgins, D. McAteer, J.C.M. Coelho, B.M. Sanchez, Z. Gholamvand, G. Moriarty, N. McEvoy, N.C. Berner, G.S. Duesberg, V. Nicolosi, J.N. Coleman, Effect of percolation on the capacitance of supercapacitor electrodes prepared from composites of manganese dioxide nanoplatelets and carbon nanotubes., ACS nano 8 (2014) 9567-79.
[15] B. Mendoza-Sánchez, T. Brousse, C. Ramirez-Castro, V. Nicolosi, P. S. Grant, An investigation of nanostructured thin film α-MoO3 based supercapacitor electrodes in an aqueous electrolyte, Electrochimica Acta 91 (2013) 253-260.
[16] Z. Yang, J. Deng, X. Chen, J. Ren, H. Peng, A Highly Stretchable, Fiber-Shaped Supercapacitor, Angewandte Chemie International Edition 52 (2013) 13453-13457.
[17] D.J. Finn, M. Lotya, G. Cunningham, R.J. Smith, D. McCloskey, J.F. Donegan, J.N. Coleman, Inkjet deposition of liquid-exfoliated graphene and MoS2 nanosheets for printed device applications, J. Mater. Chem. C 2 (2014) 925-932.
[18] G.S. Bang, K.W. Nam, J.Y. Kim, J. Shin, J.W. Choi, S.Y. Choi, Effective liquid-phase exfoliation and sodium ion battery application of MoS2 nanosheets, ACS Applied Materials and Interfaces 6 (2014) 7084-7089.

[19] J.D. Benck, T.R. Hellstern, J. Kibsgaard, P. Chakthranont, T.F. Jaramillo, Catalyzing the Hydrogen Evolution Reaction (HER) with Molybdenum Sulfide Nanomaterials, ACS Catalysis 4 (2014) 3957-3971.
[20] Q. Ding, F. Meng, C.R. English, M. Cabán-Acevedo, M.J. Shearer, D. Liang, A.S. Daniel, R.J. Hamers, S. Jin, Efficient photoelectrochemical hydrogen generation using heterostructures of Si and chemically exfoliated metallic MoS2, Journal of the American Chemical Society 136 (2014) 8504-8507.
[21] A. Harvey, C. Backes, Z. Gholamvand, D. Hanlon, D. McAteer, H.C. Nerl, E. McGuire, A. Seral-Ascaso, Q.M. Ramasse, N. McEvoy, S. Winters, N.C. Berner, D. McCloskey, J.F. Donegan, G.S. Duesberg, V. Nicolosi, J.N. Coleman, Preparation of Gallium Sulfide Nanosheets by Liquid Exfoliation and Their Application As Hydrogen Evolution Catalysts, Chemistry of Materials 27 (2015) 3483-3493.
[22] M.A. Lukowski, A.S. Daniel, F. Meng, A. Forticaux, L. Li, S. Jin, Enhanced hydrogen evolution catalysis from chemically exfoliated metallic MoS2 nanosheets, Journal of the American Chemical Society 135 (2013) 10274-10277.
[23] L. Gong, R.J. Young, I.a. Kinloch, I. Riaz, R. Jalil, K.S. Novoselov, Optimizing the reinforcement of polymer-based nanocomposites by graphene, ACS Nano 6 (2012) 2086-2095.
[24] C. Vallés, A.M. Abdelkader, R.J. Young, I.a. Kinloch, The effect of flake diameter on the reinforcement of few-layer graphene–PMMA composites, Composites Science and Technology 111 (2015) 17-22.
[25] S. Xie, O.M. Istrate, P. May, S. Barwich, A.P. Bell, U. Khan, J.N. Coleman, Boron nitride nanosheets as barrier enhancing fillers in melt processed composites, Nanoscale 7 (2015) 4443-4450.
[26] R.J. Young, I.a. Kinloch, L. Gong, K.S. Novoselov, The mechanics of graphene nanocomposites: A review, Composites Science and Technology 72 (2012) 1459-1476.
[27] C. Backes, R.J. Smith, N. McEvoy, N.C. Berner, D. McCloskey, H.C. Nerl, A. O'Neill, P.J. King, T. Higgins, D. Hanlon, N. Scheuschner, J. Maultzsch, L. Houben, G.S. Duesberg, J.F. Donegan, V. Nicolosi, J.N. Coleman, Edge and confinement effects allow in situ measurement of size and thickness of liquid-exfoliated nanosheets., Nature communications 5 (2014) 4576.
[28] M. Lotya, P.J. King, U. Khan, S. De, J.N. Coleman, High-Concentration, Surfactant- Stabilized Graphene Dispersions, ACS Nano 4 (2010) 3155-3162.
[29] O.Y. Posudievsky, O.a. Khazieieva, V.V. Cherepanov, V.G. Koshechko, V.D. Pokhodenko, High yield of graphene by dispersant-free liquid exfoliation of mechanochemically delaminated graphite, Journal of Nanoparticle Research 15 (2013) 2046.
[30] P. Atkins, J.d. Paula, Chapter 12: Rotational and vibrational spectra, Physical Chemistry, Oxford University Press, Oxford, 2014.
[31] R. Bari, D. Parviz, F. Khabaz, C.D. Klaassen, S.D. Metzler, M.J. Hansen, R. Khare, M.J. Green, Liquid phase exfoliation and crumpling of inorganic nanosheets, Phys. Chem. Chem. Phys. 17 (2015) 9383-9393.
[32] A. Ciesielski, S. Haar, M. El Gemayel, H. Yang, J. Clough, G. Melinte, M. Gobbi, E. Orgiu, M.V. Nardi, G. Ligorio, V. Palermo, N. Koch, O. Ersen, C. Casiraghi, P. Samorì, Harnessing the liquid-phase exfoliation of graphene using aliphatic compounds: a supramolecular approach., Angewandte Chemie (International ed. in English) 53 (2014) 10355-61.
[33] W. Zhang, Y. Wang, D. Zhang, S. Yu, W. Zhu, J. Wang, F. Zheng, S. Wang, J. Wang, A one-step approach to the large-scale synthesis of functionalized MoS 2 nanosheets by ionic liquid assisted grinding, Nanoscale 7 (2015) 10210-10217.
[34] J.N. Coleman, M. Lotya, A. O'Neill, S.D. Bergin, P.J. King, U. Khan, K. Young, A. Gaucher, S. De, R.J. Smith, I.V. Shvets, S.K. Arora, G. Stanton, H.-Y. Kim, K. Lee, G.T. Kim, G.S. Duesberg, T. Hallam, J.J. Boland, J.J. Wang, J.F. Donegan, J.C. Grunlan, G. Moriarty, A. Shmeliov, R.J. Nicholls, J.M. Perkins, E.M. Grieveson, K. Theuwissen, D.W. McComb, P.D. Nellist, V. Nicolosi, Two-dimensional nanosheets produced by liquid exfoliation of layered materials., Science (New York, N.Y.) 331 (2011) 568-71.
[35] K. Hashiguchi, Y. Yamakawa, Appendix A: Projection of Area, Introduction to Finite Strain Theory for Continuum Elasto-Plasticity, John Wiley & Sons, Ltd2012, pp. 385-385.
[36] R.R. Nair, P. Blake, a.N. Grigorenko, K.S. Novoselov, T.J. Booth, T. Stauber, N.M.R. Peres, a.K. Geim, Fine structure constant defines visual transparency of graphene., Science 320 (2008) 1308.

[37] C. Backes, K.R. Paton, D. Hanlon, S. Yuan, M.I. Katsnelson, J. Houston, R.J. Smith, D. McCloskey, J.F. Donegan, J.N. Coleman, Spectroscopic metrics allow in situ measurement of mean size and thickness of liquid-exfoliated few-layer graphene nanosheets, Nanoscale 8(7) (2016) 4311-23.
[38] H.-L. Liu, C.-C. Shen, S.-H. Su, C.-L. Hsu, M.-Y. Li, L.-J. Li, Optical properties of monolayer transition metal dichalcogenides probed by spectroscopic ellipsometry, Applied Physics Letters 105 (2014) 201905.
[39] V. Vega-Mayoral, C. Backes, D. Hanlon, U. Khan, Z. Gholamvand, M. O'Brien, G.S. Duesberg, C. Gadermaier, J.N. Coleman, Photoluminescence from Liquid-Exfoliated WS2 Monomers in Poly(Vinyl Alcohol) Polymer Composites, Advanced Functional Materials 26(7) (2016) 1028-1039.
[40] Y. Arao, M. Kubouchi, High-rate production of few-layer graphene by high-power probe sonication, Carbon (2015).
[41] M. Ayán-Varela, J.I. Paredes, L. Guardia, S. Villar-Rodil, J.M. Munuera, M. Díaz-González, C. Fernández-Sánchez, A. Martínez-Alonso, J.M.D. Tascón, Achieving Extremely Concentrated Aqueous Dispersions of Graphene Flakes and Catalytically Efficient Graphene-Metal Nanoparticle Hybrids with Flavin Mononucleotide as a High-Performance Stabilizer, ACS Applied Materials & Interfaces (2015) 150506130806005.
[42] U. Khan, A. O'Neill, M. Lotya, S. De, J.N. Coleman, High-concentration solvent exfoliation of graphene., Small (Weinheim an der Bergstrasse, Germany) 6 (2010) 864-71.
[43] S. Lin, C.-J. Shih, M.S. Strano, D. Blankschtein, Molecular insights into the surface morphology, layering structure, and aggregation kinetics of surfactant-stabilized graphene dispersions., Journal of the American Chemical Society 133 (2011) 12810-23.
[44] M. Lotya, Y. Hernandez, P.J. King, R.J. Smith, V. Nicolosi, L.S. Karlsson, F.M. Blighe, S. De, Z. Wang, I.T. McGovern, G.S. Duesberg, J.N. Coleman, Liquid phase production of graphene by exfoliation of graphite in surfactant/water solutions., Journal of the American Chemical Society 131 (2009) 3611-20.
[45] P. May, U. Khan, J.M. Hughes, J.N. Coleman, Role of Solubility Parameters in Understanding the Steric Stabilization of Exfoliated Two-Dimensional Nanosheets by Adsorbed Polymers, The Journal of Physical Chemistry C 116 (2012) 11393-11400.
[46] D. Nuvoli, L. Valentini, V. Alzari, S. Scognamillo, S.B. Bon, M. Piccinini, J. Illescas, A. Mariani, High concentration few-layer graphene sheets obtained by liquid phase exfoliation of graphite in ionic liquid, Journal of Materials Chemistry 21 (2011) 3428.
[47] A. O'Neill, U. Khan, J.N. Coleman, Preparation of high concentration dispersions of exfoliated MoS 2 with increased flake size, Chemistry of Materials 24 (2012) 2414-2421.
[48] R.J. Smith, P.J. King, M. Lotya, C. Wirtz, U. Khan, S. De, A. O'Neill, G.S. Duesberg, J.C. Grunlan, G. Moriarty, J. Chen, J. Wang, A.I. Minett, V. Nicolosi, J.N. Coleman, Large-Scale Exfoliation of Inorganic Layered Compounds in Aqueous Surfactant Solutions, Advanced Materials 23 (2011) 3944 - 3948.
[49] L. Xu, J.W. McGraw, F. Gao, M. Grundy, Z. Ye, Z. Gu, J.L. Shepherd, Production of high-concentration graphene dispersions in low-boiling-point organic solvents by liquid-phase noncovalent exfoliation of graphite with a hyperbranched polyethylene and formation of graphene/ethylene copolymer composites, Journal of Physical Chemistry C 117 (2013) 10730-10742.
[50] M. Yi, Z. Shen, X. Zhang, S. Ma, Achieving concentrated graphene dispersions in water/acetone mixtures by the strategy of tailoring Hansen solubility parameters, Journal of Physics D: Applied Physics 46 (2013) 025301.
[51] L. Zhang, Z. Zhang, C. He, L. Dai, J. Liu, L. Wang, Rationally Designed Surfactants for Few-Layered Graphene Exfoliation: Ionic Groups Attached to Electron-Deficient π-Conjugated Unit through Alkyl Spacers., ACS nano 8 (2014) 6663-70.
[52] R. Zhang, B. Zhang, S. Sun, Preparation of high-quality graphene with a large-size by sonication-free liquid-phase exfoliation of graphite with a new mechanism, RSC Adv. 5 (2015) 44783-44791.